Optical design of the *Origins* space telescope

James A. Corsetti[a], Edward G. Amatucci[a], Ruth C. Carter[a], Tom D'Asto[b],
Michael J. DiPirro[a], Benjamin Gavares[c], Joseph M. Howard[a],
David T. Leisawitz[a], Gregory E. Martins[a], Margaret Meixner[d], and Len Seals[a]
[a]NASA GSFC, 8800 Greenbelt Rd, Greenbelt, MD 20771;
[b]ATA Aerospace, 7474 Greenway Center Dr, Suite 500, Greenbelt, MD 20770
[c]Northrup Grumman, 5010 Herzel Pl, Beltsville, MD 20705
[d]STScI, 3700 San Martin Dr, Baltimore, MD 21218

ABSTRACT

This paper discusses the optical design of the *Origins Space Telescope*. *Origins* is one of four large missions under study in preparation for the 2020 Decadal Survey in Astronomy and Astrophysics. Sensitive to the mid- and far-infrared spectrum (between 2.8 and 588 μm), *Origins* sets out to answer a number of important scientific questions by addressing NASA's three key science goals in astrophysics.

The *Origins* telescope has a 5.9 m diameter primary mirror and operates at *f*/14. The large on-axis primary consists of 18 'keystone' segments of two different prescriptions arranged in two annuli (six inner and twelve outer segments) that together form a circular aperture in the goal of achieving a symmetric point spread function. To accommodate the 46 x 15 arcminute full field of view of the telescope at the design wavelength of λ = 30 μm, a three-mirror anastigmat configuration is used. The design is diffraction-limited across its instruments' fields of view. A brief discussion of each of the three baselined instruments within the Instrument Accommodation Module (IAM) is presented: 1) *Origins* Survey Spectrometer (OSS), 2) Mid-infrared Spectrometer, Camera (MISC) transit spectrometer channel, and 3) Far-Infrared Polarimeter/Imager (FIP). In addition, the upscope options for the observatory are laid out as well including a fourth instrument: the Heterodyne Receiver for *Origins* (HERO).

Keywords: Optics, *Origins*, infrared, segmented mirror, Decadal, imaging, spectroscopy, polarimetry

1. INTRODUCTION

We note that portions of this manuscript appear in the *Origins* Study Final Report.

Origins is one of four large missions currently under study for the 2020 Decadal Survey in Astronomy and Astrophysics.[1-2] Sensitive in the mid- and far-infrared spectrum (between 2.8 and 588 μm) and set to launch in approximately 2035, *Origins* is designed to address NASA's three key astrophysics science goals: How does the universe work?, How did we get here, and Are we alone? To do so, *Origins* seeks to answer three main questions:

1) How do galaxies form stars, build up metals, and grow their central supermassive black holes from reionization to today?
2) How do the conditions for habitability develop during the process of planet formation?
3) Do planets orbiting M-dwarf stars support life?

As shown in Figure 1, *Origins* has a Spitzer-like architecture with fixed baffles and simplified deployment for the sun shields. The observatory is designed with a modular instrument bay that facilitates integration and test and allows potential serviceability of the current instruments or potential replacement with new ones. Figure 1 shows the telescope itself with the science instruments sitting directly behind the primary mirror. The locations of the spacecraft, solar array, and deployed sun shield are indicated as well.

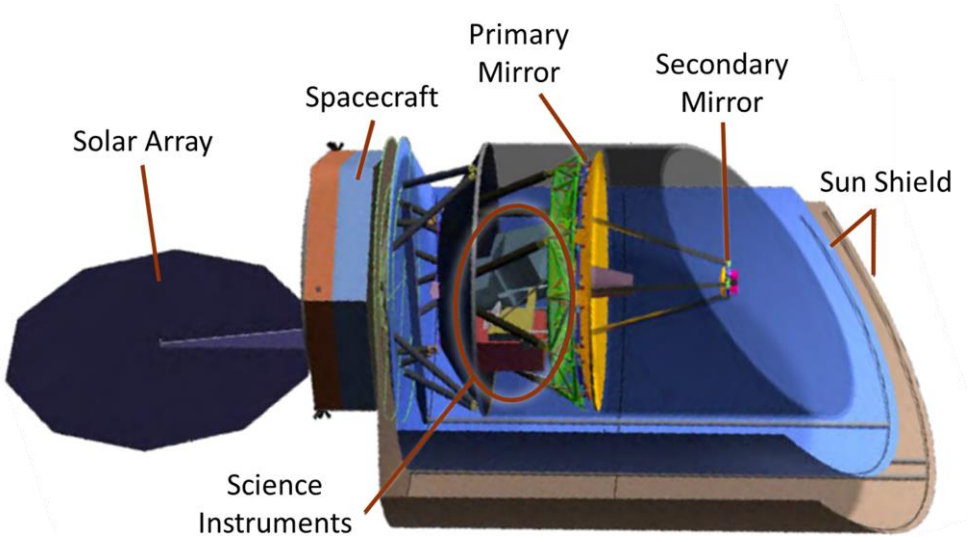

Figure 1. Structural model of the *Origins* space telescope observatory

2. TELESCOPE OPTICAL DESIGN

2.1 Design Form

As shown in Figure 2, the *Origins* telescope is a three mirror anastigmat (TMA) with a field-steering mirror. This four mirror design includes three mirrors with optical power (the elliptical primary, hyperbolic secondary, and elliptical tertiary mirrors) and a flat FSM. The TMA is the same general optical design form that has been proven on JWST and is therefore well understood and low risk. An initial, off-axis optical design considered for *Origins* resulted in a TMA with a "freeform" surface on all four mirrors to assist in correction of optical aberrations. Later studies found these design aspects to be costly and more challenging to implement, and so the design was modified. Other benefits of choosing the on-axis architecture over the off-axis one include avoiding a secondary mirror that requires deployment on orbit, as well as allowing the instrument volume to fit compactly behind the primary mirror. As such, the final baseline design was constrained to have an on-axis pupil (obstructed primary mirror) with the remaining three mirrors simple on-axis conics. The obstructed primary mirror also made the observatory simpler to package in the fairing as compared to studies regarding a telescope with an unobstructed primary mirror. While a number of aperture shapes were investigated for the purpose of this design study (based on the goal of trying to find the one easiest to package and deploy), ultimately a circular aperture was chosen as it yielded the point spread function (PSF) with the least effects of diffraction while being possible to fit it already fully-deployed within the chosen fairing before launch. This fact is a major benefit of the telescope design as the lack of deployments leads to lower risk and reduced cost. Requirements for the *Origins* telescope are summarized in Table 1.

The primary mirror has 18 segments and is *f*/0.63 as shown in Table 1. A fast primary mirror is desirable for shortening the distance between the vertices of the primary and secondary mirrors (being approximately 3.33m in the current design), therefore reducing the overall size of the observatory. Between the secondary and tertiary mirrors, the rays form an internal image (Cassegrain focus) that allows the tertiary mirror to image a real exit pupil. This real image will be surrounded by baffling to reject stray light. The FSM is placed at the exit pupil of the telescope, which actively tilts to control the field of view (FOV), directing it into each instrument as the observatory slowly drifts over the course of an observation. The telescope image surface is concave, with its center of curvature located at the FSM surface. Placing the FSM at the exit pupil (which is also at the center of curvature of the telescope image surface) prevents defocus from occurring during tilting of the FSM. This effectively makes a locally-telecentric system for each field point, for which each chief ray is normal to the curved image surface.

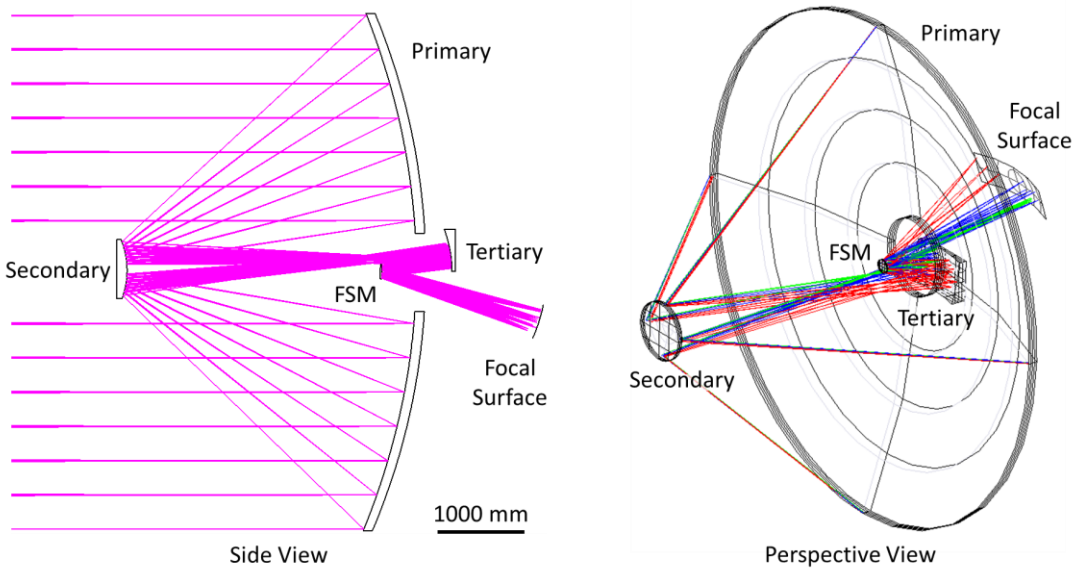

Figure 2. *Origins* baseline telescope layout shows the locations of the four mirrors and focal surface from both side (left) and perspective (right) views.

Table 1. Design requirements for the *Origins* space telescope

Parameter	Origins Baseline	Units
Primary Size	Circular, 5.9	Meters
f-number	*f*/14.0 (telescope) *f*/0.63 (primary)	--
Effective Focal Length	82.6	Meters
Field of View	46 x 15	Arcmin
Waveband	2.8 - 588	Microns
Operating Temp.	4.5	Kelvin
Optical Performance	Diffraction limited at λ = 30 μm	
Design Form	Three Mirror Anastigmat Obstructed (on-axis pupil)	
Mirror Coatings	Protected Gold	
Optical and Structural Material	Beryllium O-30	

Each mirror is assumed to be made of beryllium O-30-H with a density of 1.85 g/cm^3. This material was chosen due to its high stiffness, low density, low coefficient of thermal expansion, and high thermal conductivity and is baselined for the optical components and instrument structures throughout the observatory. Figure 3 shows dimensions for the six inner and twelve outer "keystone" segments that make up the primary mirror. Because the primary mirror is on-axis, all of the outer segments are identical. The inner segments have identical optical prescriptions; however, two variants are needed to accommodate a notch for the secondary mirror struts. Three of the inner mirror segments match the outline shown in Figure 3, and three segments are reflections of this shape, with the notch in the opposite corner. All four mirrors are gold-coated for improved reflectance in the infrared. Each mirror coating is assumed to have 98% reflectance and 2% emissivity, which is consistent with measurements made on JWST's protected gold-coated mirrors up to a wavelength of 29μm.[3] Non-JWST measurements on protected gold coatings in the terahertz regime have reported

reflectance values around 99% between 100 and 600 µm.[4] Based on this the total throughput for the *Origins* telescope is at least 92% with higher throughput at longer wavelengths.

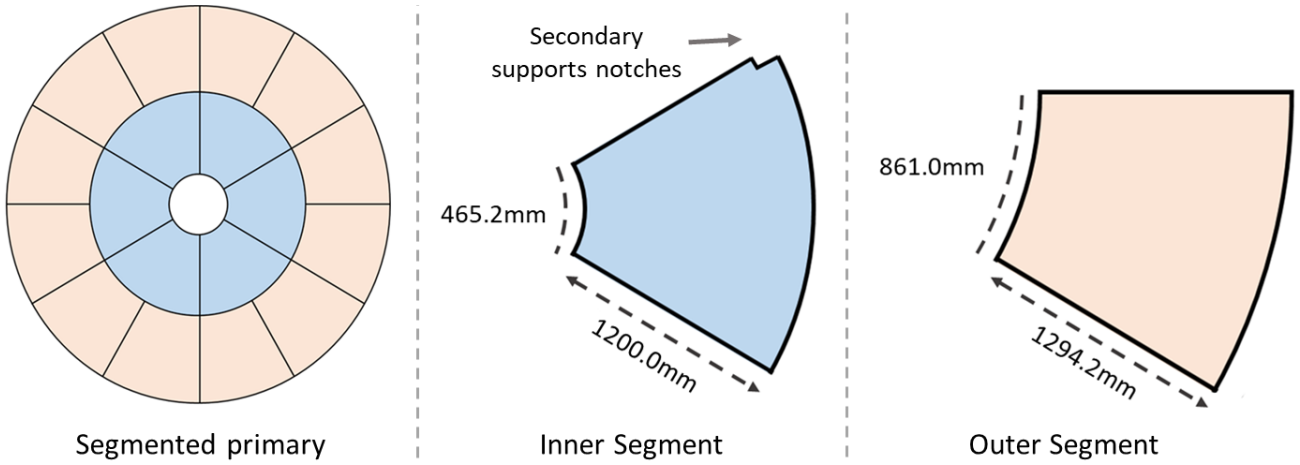

Figure 3: The twelve *Origins* primary mirror outer segments are identical. The inner segments are of the same optical prescription, but with two variants on the location of the secondary support notch.

2.2 Imaging Performance

The *Origins* telescope is required to be diffraction-limited at a wavelength of 30 µm. Root-mean-square (RMS) wavefront error is taken to be the metric by which performance is evaluated. A common standard for diffraction-limited performance is to have less than 0.07 λ of wavefront error. For a design wavelength of 30 µm, this corresponds to less than 2.1 µm RMSWE. Figure 4 shows that this specification is met across the telescope's and therefore each instrument's FOV. Note that the field of view is not symmetric around 0° in the x field direction. The reason for this is explained in further detail in the instruments section of this paper.

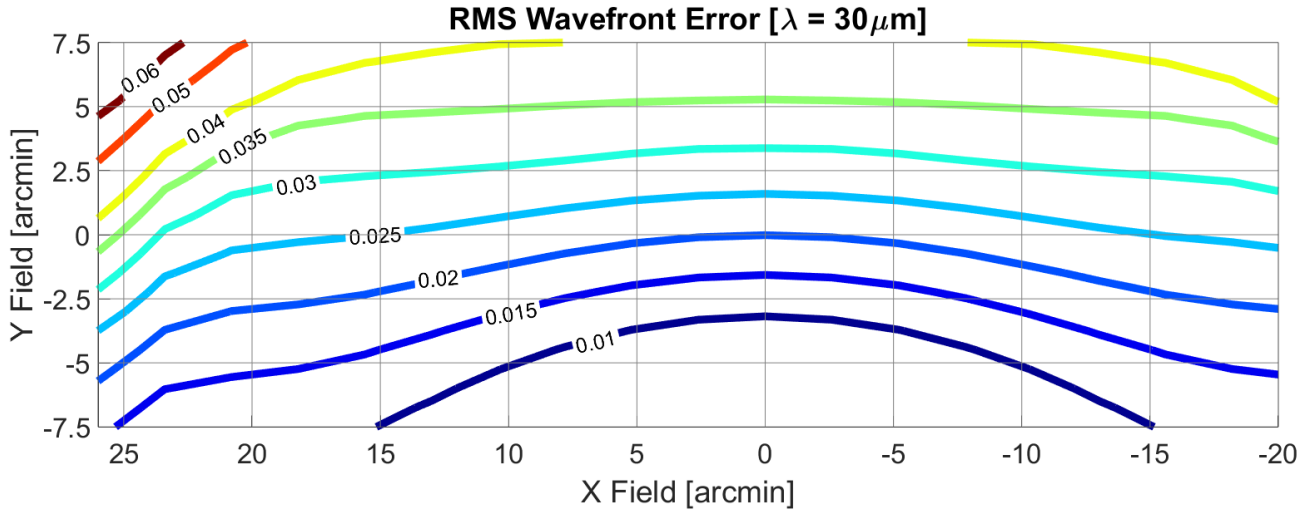

Figure 4. Contour plot showing RMS wavefront error as a function of field-of-view for the *Origins Space Telescope*. Contours are plotted in regular increments to indicate that all values are below the required 0.07 λ of wavefront error.

2.3 Stray light analysis

Stray light analysis refers to the process of identifying and preventing light rays from any source other than the object being observed, from reaching the detector plane. For this purpose, mechanical structures known as baffles are incorporated into the telescope design to block these unwelcome rays' potential "skip paths." Tight packaging constraints require careful consideration of how to adequately baffle against stray light. Often the constraints involved make it difficult to achieve well separated paths from image and pupil conjugates, which would permit placement of effective baffles. As a result, baffling may be limited to careful use of pupil masks and baffles combined with field masks at or near intermediate images to restrict specular paths from the sky to the focal plane other than from within the field of view. The stray light analysis of *Origins* was carried out in FRED software.

Figure 5 shows *Origins*' external and internal baffling. The external baffling is shown in red in the image on the left while the image on the right shows the 'snout' baffling and vanes that are coming away from the hole in the primary mirror towards the secondary mirror. Figure 6 shows the effectiveness of the baffling in blocking stray light. In each case, rays were traced backwards through the system from the instrument FOV footprints at the focal surface towards the primary and onto the sky. In Figure 6, the rays leaving the focal surface are colored green and remain so until reflecting off of the tertiary mirror, at which point they are colored red. In the top picture (without baffling) there is a significant ray path that allows light to travel directly from the focal surface to the sky without hitting the tertiary (as evident from the fact that the rays remain green in color). In the bottom picture, the baffling blocks this skip path and only the desired FOV (the red rays) make it all the way from the image surface to the sky. Figure 7 shows the intensity signal to noise ratio between the desired FOV allocated to the instruments and noise due to scatter. Figure 7 shows that the difference between the two is between about four and five orders of magnitude. This value can be further reduced by adding further baffles. As the FSM is located at the exit pupil of the telescope, an image of the primary mirror forms there. To further mitigate stray light, it is useful to place a baffle around the FSM, as was the case for the FSM of JWST.

In addition to blocking skip paths as mentioned above, scatter is another consideration in stray light analysis. Scatter can be reduced by using mirrors that are well polished with low surface roughness as well as clean. In the FRED model, surface roughness is represented by the Harvey-Shack model with particulate contamination modeled by MIL-STD-1246C. Figure 8 shows the effect of surface roughness in more detail. By increasing the surface roughness of the primary mirror from 1.5 to 15 to 100nm (while leaving the secondary, tertiary, and FSM each with a surface roughness of 1.5nm in each case) it is apparent that a rougher surface leads to a worsened signal to noise ratio between on and off-axis. This is due to the increased scatter. The bottom plot of Figure 8 shows the case for which the primary mirror has again a surface roughness of 1.5nm but no longer includes any baffling. Further design studies will determine the final requirements on surface roughness. In order to limit thermal radiation from the telescope, a combination of high-emissivity materials/coatings and low temperature is employed throughout the design of the observatory. The cooling system utilizes a combination of passive cooling provided by a two-layer deployed sunshield, a single stage radiator at 35 K, and four mechanical cryocoolers in operating in parallel. The thermal design of *Origins* enables a transition between 280 K at the outer sunshield, 119 K at the inner sunshield, 35 K at the barrel, 20 K at the middle zone, and 4.5 K for the instruments and telescope. For more information on the thermal design, please see the *Origins* final report.

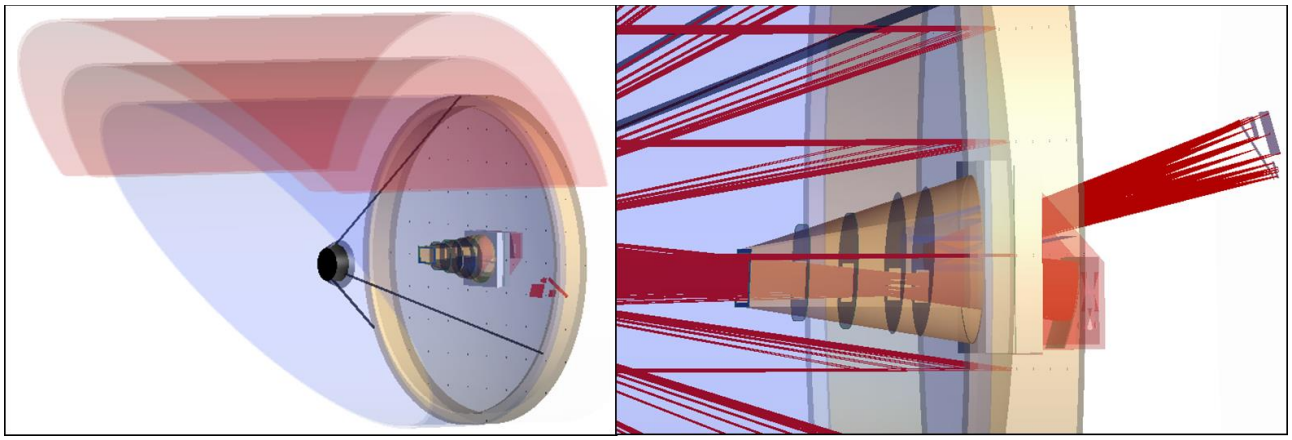

Figure 5. External (left) and internal (right) baffles. Both sets of baffling are meant to prevent unwanted light from reaching the focal surface.

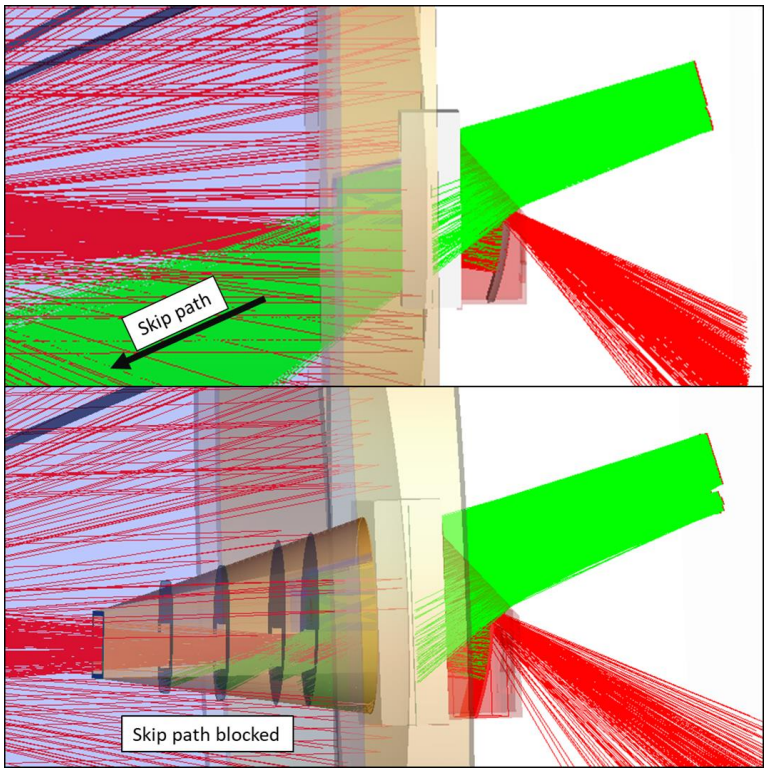

Figure 6. Images showing the effect of baffling to mitigate stray light. (Top) No baffling allows for skip ray paths and light to travel directly from the sky to focal surface without reflecting off the telescope mirrors versus (bottom) having baffling which prevents this from occurring.

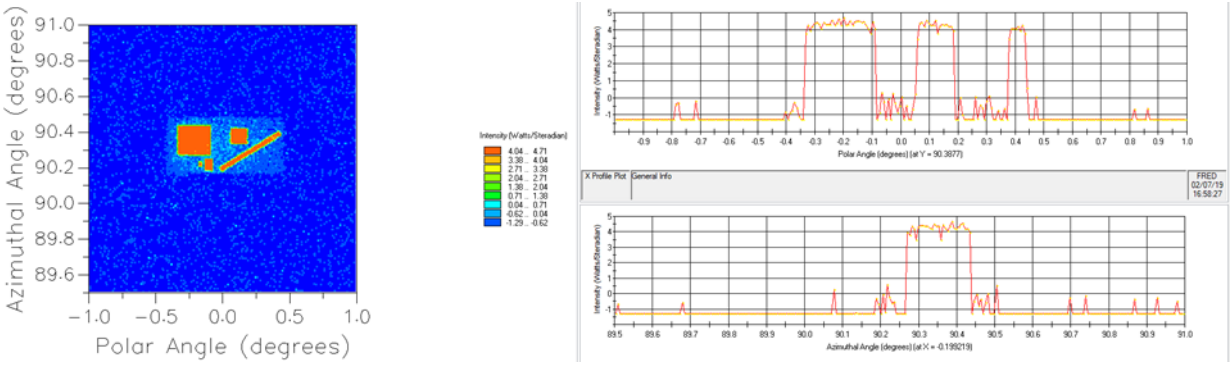

Figure 7. Analysis showing relative intensity between the desired signal (the instruments' FOV footprints) and noise due to near-field scatter. Note that the x and y line scans are plotted on a logarithmic scale and show between about four and five orders of magnitude difference between signal and noise. Calculations carried out at $\lambda = 30\mu m$.

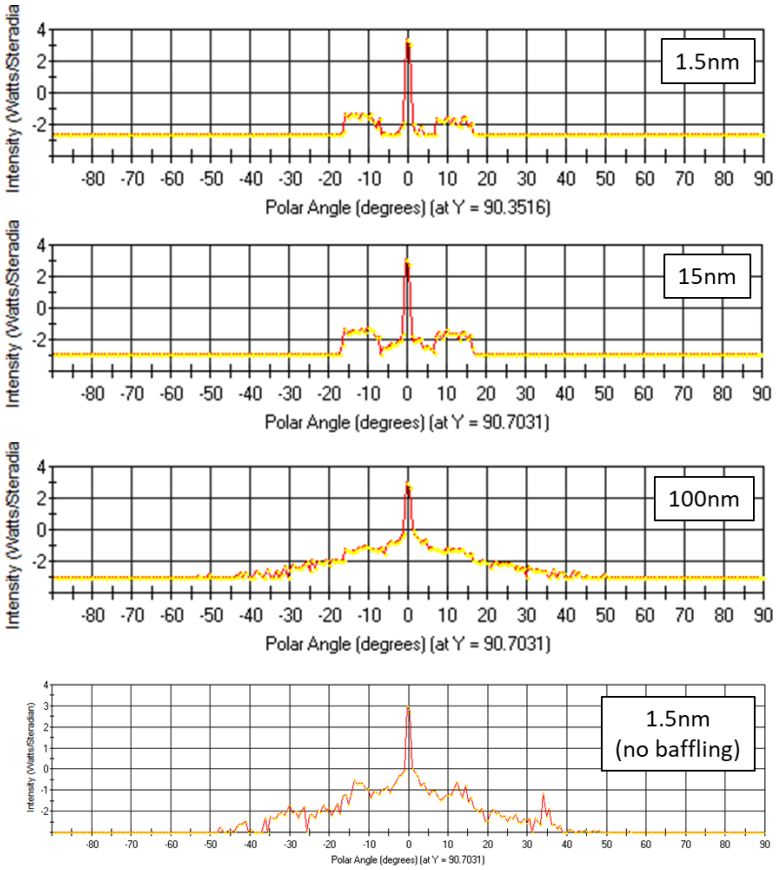

Figure 8. The effect of primary mirror surface roughness on intensity as a function of FOV angle. As expected, as the primary mirror surface roughness increases, more scatter occurs from the surface, worsening the signal to noise ratio between on and off-axis. Note that the intensity scales are logarithmic. Calculations carried out at $\lambda = 30\mu m$.

3. INSTRUMENTS

The baseline *Origins* design contains three instruments. These are: 1) the *Origins* Survey Spectrometer (OSS)[5], 2) Mid-infrared Spectrometer, Camera transit spectrometer channel (MISC-T)[6-7], and 3) Far-Infrared Polarimeter/Imager (FIP)[8]. OSS is the primary science instrument with six grating modules to enable simultaneous spectroscopic measurements between 25 and 588μm at a resolving power (R) of 300. In addition to the grating modules, OSS provides two high resolution modes: a Fourier-Transform Spectrometer and an etalon which enable R = 30,000 and R = 200,000 measurements, respectively, over narrower spectral ranges. MISC is a densified pupil spectrometer that provides R values between 50 and 295 over a spectral range between 2.8 and 20 μm for transiting exoplanet spectroscopy with very high spectro-photometric stability. FIP serves the role of the observatory's large field-of-view imager, providing both traditional imaging and polarimetry measurements.

Figure 9 shows the field of view allocations for each of the three baselined instruments. As mentioned previously, the telescope is designed over a rectangular 15 x 46 arcminute full FOV; however, this FOV is not symmetric, being longer in the direction of OSS than FIP. This is due to the fact that during the design process, further FOV was added to OSS after the FIP design had been completed. Rather than redesign FIP at that stage, OSS's FOV was extended in the direction away from the center of the FOV. This asymmetry can be addressed in a later design by just shifting both instruments' designated FOVs by approximately 3 arcminutes. In Figure 9, one arcminute of FOV on the sky corresponds to about 24 mm in length at the focal surface. Space for mounting structures is left between the instruments. Looking at Figure 9, there is a large amount of space between the different instruments in the x direction of the FOV. This is to make it possible to more easily accommodate any desired upscopes to the *Origins* baseline design. Optional Upscopes include: greater FOV for both OSS and FIP, another channel for MISC, and the addition of the HERO instrument. In future design iterations, once the total number of instruments and FOV allocations for each instrument is

decided, the footprints in Figure 9 would be reoptimized to make better use of the central 'sweet spot' of optical performance and reduce the large gaps between instruments. Figure 10 shows a CODEV® layout showing rays for each of the three baseline instruments passing through the telescope onto the image surface.

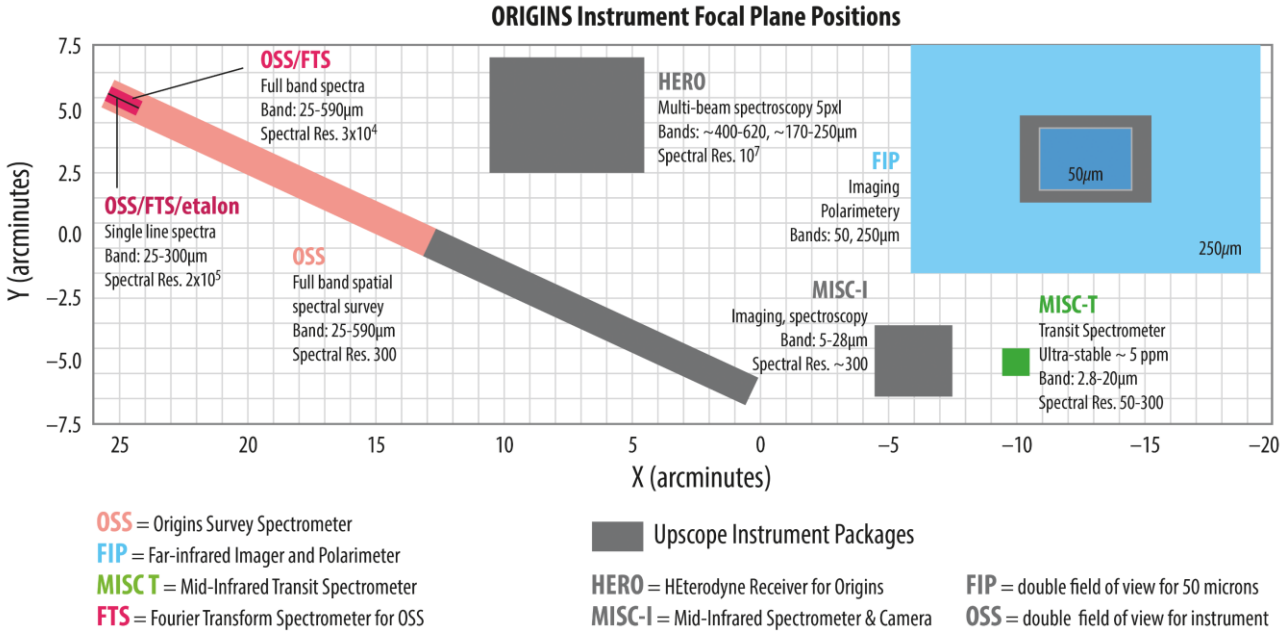

Figure 9. Field of view allocations for each of the *Origins* instruments.

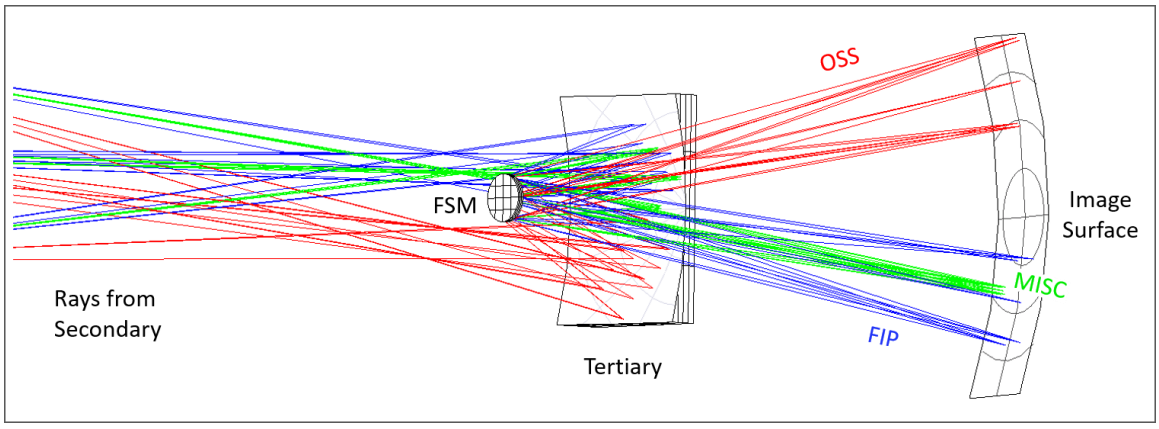

Figure 10. Ray trace showing the light reflecting from the FSM to *Origins* image surface and individual instruments.

4. CONCLUSIONS

In this paper, we presented an overview of the *Origins Space Telescope* observatory and the associated optical design. Details regarding optical performance including RMS wavefront error and stray light are presented, alongside an introduction to the *Origins* instruments. For more information on these topics, the reader is encouraged to read the *Origins* Final Report, which details the results of this study (see the Documents link on reference [1]).

REFERENCES

[1] *Origins* Space Telescope. NASA Goddard. https://asd.gsfc.nasa.gov/firs/

[2] Leisawitz, D., “The Origins Space Telescope” Proc. SPIE 11115, UV/Optical/IR Space Telescopes and Instruments: Innovative Technologies and Concepts IX, 11115-25, (2019)
[3] Keski-Kuha, R.A., Bowers, C.W., Quijada, M.A., et al., “James Webb Space Telescope optical telescope element mirror coatings," Proc. SPIE 8442, Space Telescopes and Instrumentation 2012: Optical, Infrared, and Millimeter Wave, 84422J (2012);
[4] Naftaly, M. and Dudley, R., "Terahertz reflectivities of metal-coated mirrors," Appl. Opt. 50, 3201-3204 (2011)
[5] Bradford, C.M., Cameron, B., Moore, B., et al., "The Origins Survey Spectrometer (OSS): a far-IR discovery machine for the Origins Space Telescope," Proc. SPIE 10698, Space Telescopes and Instrumentation 2018: Optical, Infrared, and Millimeter Wave, 1069818 (2018)
[6] Matsuo, T., Satoshi, I., Shibai, H., Takahiro, S., and Yamamuro, T. “A New Concept for Spectrophotometry of Exoplanets with Space-borne Telescopes,” ApJ, 823, 139 (2016)
[7] Sakon, I., Roellig, T.L., Ennico-Smith, K., et al., "The mid-infrared imager, spectrometer, coronagraph (MISC) for the Origins Space telescope (OST)," Proc. SPIE 10698, Space Telescopes and Instrumentation 2018: Optical, Infrared, and Millimeter Wave, 1069817 (2018)
[8] Staguhn, J., Amatucci, E., Armus L., et al., "Origins Space Telescope: the far infrared imager and polarimeter FIP," Proc. SPIE 10698, Space Telescopes and Instrumentation 2018: Optical, Infrared, and Millimeter Wave, 106981A (2018)